TECHNICAL ARTICLE

Effect of Phosphorus Content on Properties of Warm-Rolled Interstitial-Free Steel Sheets

Wei-min Guo · Zuo-cheng Wang · Yong-de Li · Na Xu · Jun-bo Shi

Abstract Microstructures, precipitates, and textures of experimental phosphorus additions to high-strength and traditional Ti-bearing interstitial-free (IF) steels were evaluated by uniaxial tensile test, transmission electron microscope and electron backscatter diffraction. The results show that IF steel is strengthened significantly by addition of phosphorus. Yield strength increases by 60 MPa, from 105 to 165 MPa; and tensile strength increases by 80 MPa, from 245 to 325 MPa. Phosphorus impairs formability while improving strength. Elongation, n value (work hardening), and r value (transverse strain/ vertical anisotropy) are decreased from 50%, 0.31, and 1.75 to 40%, 0.25, and 1.38, respectively. Research shows that phosphorus degradation in steel is due to two mechanisms: (1) high-temperature aging and formation of FeTiP particles, and (2) solid-solution strengthening and the role FeTiP particles play in blocking nucleation and growth of textures in the {111} orientation. This results in a weak, annealed {111} texture, so that the r value decreases.

Keywords High-strength IF steel · Precipitates · FeTiP · r Value · Texture

W. Guo (✉) · Y. Li · N. Xu · J. Shi
Shandong Province Material Failure Analysis and Safety Assessment of Engineering Technology Center, Shandong Analysis and Test Center, Shandong Academy of Sciences, Jinan 250014, People's Republic of China
e-mail: gweimin84@gmail.com

W. Guo · Z. Wang
School of Materials Science and Engineering, Shandong University, Jinan 250061, People's Republic of China

Introduction

Over the last two decades, interstitial-free high-strength (IFHS) steels have become more widely utilized in the automotive industry because of their excellent deep drawability, coupled with adequate strength [1]. IFHS steels containing P or Mn are among the most important interstitial-free (IF) steels for the automotive industry [2]. These alloys are strengthened by solid-solution hardening [3]. Research has shown that P has a stronger solid-solution strengthening effect than Mn and Si, due to decreased degradation of deep drawability and lower cost [4]. Phosphorus is used more widely than Mn and Si in IFHS; however, the deep drawability of IFHS is inferior to normal IF steels [5]. It is important to understand how P reacts in steels to produce IFHS with adequate deep drawability.

Warm-rolling technology has been rapidly developed in many countries because it has the potential to broaden the product range and decrease cost of hot-rolling strip. Barnett et al. [6] concluded in 1996 that warm-rolled steel may be more readily used to replace cold-rolled strip in the case of IF products. Jonas [7] reported that warm rolling has gained in popularity among steelmakers as a means of cutting the cost of steel production and opening up the window of hot band properties. Guan et al. [8], Guo et al. [9], and Wang et al. [10] have reported similar findings using warm rolling. Warm rolling also has an advantage in that beneficial textures can be developed to improve deep drawability, especially in the production of warm-rolled IF steel [11, 12]. The warm-rolling process, where steels are rolled at temperatures within the ferrite region (650–800 °C) [13], has become a major means of producing hot-rolled IF steel [14, 15].

Precipitates play an important role in the properties of IF steels. Small precipitated particles, which are detrimental

Table 1 Composition analysis of experimental steels (wt%)

Steel	C	Si	Mn	P	S	Al	N	Ti	Ti^{exc}
Ti-IF	0.002	0.008	0.16	0.002	0.004	0.019	0.0029	0.072	0.048
Ti + P-IF	0.002	0.005	0.16	0.085	0.0026	0.023	0.0021	0.065	0.0459

Table 2 Mechanical properties of experimental steels

Steel	TS/TF (°C)	Red (%)	YS (MPa)	TS (MPa)	El (%)	n Value	r Value
Ti-IF	700/560	90	105	245	50	0.31	1.75
Ti + P-IF	700/560	90	165	325	40	0.25	1.38

for texture development, will block the migration of crystal boundaries and further lower the r value [16].

In this article, a warm-rolled high-strength IF steel containing phosphorus is studied by examining the microstructure to identify the precipitates, measure the texture, and correlate the microstructural features to the mechanical properties to determine the role of phosphorus in these alloys.

Experimental Material and Procedures

Experimental Materials

The materials used in this study are Ti-stabilized high-strength IF steel with P addition (Ti + P-IF) and ordinary Ti-stabilized IF steel (Ti-IF). Chemical compositions are listed in Table 1.

Note: $\mathrm{Ti}^{exc} = \mathrm{Ti} - \dfrac{48}{12}\mathrm{C} - \dfrac{48}{14}\mathrm{N} - \dfrac{48}{32}\mathrm{S}$

where Ti, C, N, and S are the content of each element in steel; Ti^{exc} is the Ti content that is not alloyed.

Experimental Procedure

The alloys were melted in a vacuum induction furnace. The 500 kg-ingots were forged and cut into plates for hot rolling. The final thickness of forged plates was 30 mm. Billet reheating was achieved in an electric heating furnace. The plates were austenitized at 1050 °C for 2 h and air cooled to 700 °C (TS), and rolled through four passes in the ferrite region. Total reduction was 90%. Finish rolling temperature (TF) of both warm-rolled steel sheets was about 560 °C. After rolling in the ferrite region, the sheets were air cooled to room temperature and then batch annealed at 750 °C for 3 h. In a documented study [17], it is indicated that, without lubrication, the inhomogeneity of the microstructure in the thickness direction in hot-rolled plate still exists after annealing. In contrast, with lubrication, the steel sheet deformed homogeneously in the thickness direction, and hot-rolled and annealed microstructures were distributed evenly in the thickness direction; furthermore, the steel exhibited good deep drawability after hot rolling and annealing. The lubrication oil is a type of grease that is composed of solid lubricant, high-temperature synthetic agent, and inorganic lubricant. Warm-rolling experiments were carried out in a two-roller reversible-type mill; diameter, length, and rolling speed of the roller were 300 mm, 350 mm, and 75 rpm, respectively.

Tensile test was carried out according to the ISO 6892-1: 2009 [18] standard. Samples from the annealed warm-rolled steel sheets were cut and machined into tensile specimens; mechanical properties were all measured by a uniaxial tensile test. The tensile specimen tests of all groups were conducted in triplicate, in three directions, at angles of 0°, 45°, and 90° to the rolling direction (RD). Results for each direction were recorded as the average of the three specimens. Mechanical properties were calculated using formula $X = (X_0 + 2X_{45} + X_{90})/4$. In addition, r values and n values were tested according to ISO 10113: 2006 [19] and ISO 10275: 2007 [20].

Transmission electron microscope (TEM) analysis was carried out using both thin foils and carbon extraction replicas. The TEM used in this study was operated at 150 kV. Electron backscatter diffraction (EBSD) was used to produce orientation maps of the RD and traverse direction sections of the two experimental steels. In consideration of the fact that textures may be different from surface to center of the rolled steels, EBSD data were collected from the 1/4-thickness layer from surface. Orientation maps were acquired using a field emission scanning electron microscope (FESEM). An accelerating voltage of 20 kV and a 60-µm aperture were used. The sections were positioned at a working distance of 25 mm with a tilt of 70°. The orientation maps were processed by using *HKL Technology Channel 5* software.[1]

---

[1] HKL Technology Channel 5: EBSD system which will allow imaging, diffraction pattern acquisition, and indexing, phase identification, orientation mapping, determination of pole figures, and orientation distribution function (ODF) calculations (HKL TECHNOLOGY INC., Denmark).

Experimental Results

Mechanical properties of experimental steels are shown in Table 2. As illustrated in Fig. 1, the steel is strengthened by the presence of phosphorus. Yield strength increases by 60 MPa, from 105 to 165 MPa and tensile strength rises by 80 MPa, from 245 to 325 MPa. However, formability is impaired as a result of the P addition. Elongation decreases from 50 to 40%, and the n value and r value drop from 0.31 and 1.75 to 0.25 and 1.38, respectively.

Figure 2 shows the microstructures of annealed (750 °C/ 3 h) ordinary Ti-IF steel and high-strength Ti + P-IF steels. It can be seen that Ti-IF steel is completely recrystallized, and the grains are equiaxed; while grains are elongated in the high-strength steel with P addition.

Observations show that precipitates in high-strength steel with P-addition are similar to those in ordinary Ti-IF steels. As shown in Figs. 3 and 4, there are $Ti_4C_2S_2$, TiS, and TiN particles in both high-strength and ordinary Ti-IF steels. Figure 5 shows fine FeTiP particles, with a crystallographic orientation in high-strength Ti + P-IF steel. These precipitates do not form in ordinary Ti-IF steel.
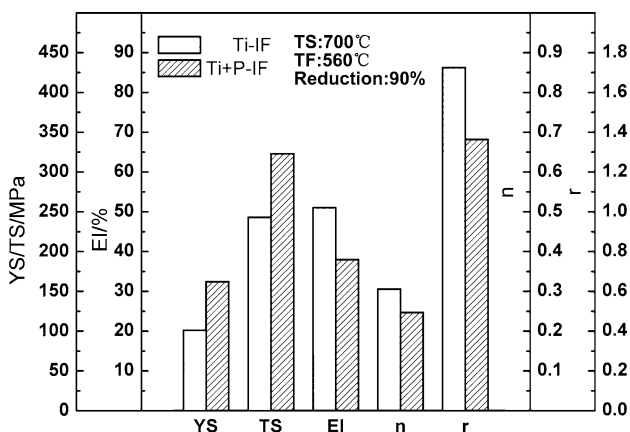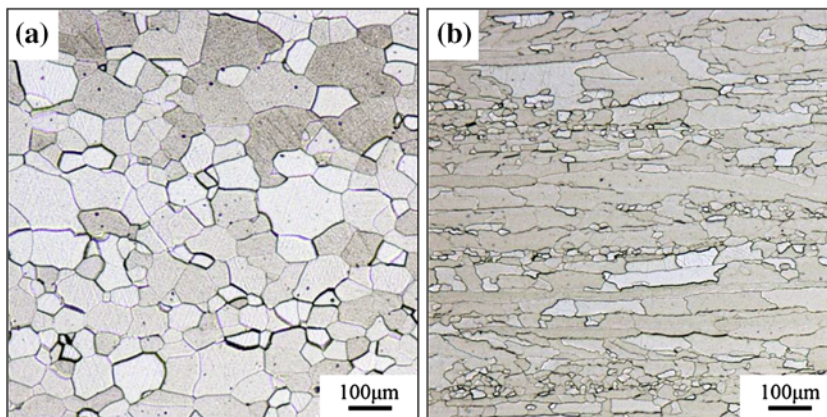
TEM observations also identified some compound precipitates in high-strength Ti + P-IF steel, as shown in Fig. 6(a). This is the compound precipitate of $Ti_4C_2S_2$ and TiS. A small number of Fe_4N particles were found in thin film specimens, as shown in Fig. 6(b) and (c).

Figure 7 shows the ODF maps of the two experimental steels before annealing ($\varphi_2 = 45°$). Figs. 8 and 9 show the $\varphi_2 = 45°$ section ODF maps and orientation density change along (a) α, (b) γ, and (c) ε fibers. It is shown that both warm-rolled Ti-IF steel and Ti + P-IF steel have strong α and γ textures. The α and γ textures in high-strength Ti + P-IF steel are stronger than those in Ti-IF steel. However, after annealing, γ texture in Ti-IF steel is greatly strengthened while the good textures in high-strength Ti + P-IF steels are changed slightly. As a result, high-strength Ti + P-IF steel has weaker deep drawability than Ti-IF steel.

Discussion

The recrystallization temperature is raised by the presence of P in the alloy and complete recrystallization occurs at a temperature above 750 °C. As shown in Fig. 2, annealed ordinary Ti-IF steel has completely recrystallized and exhibits an equiaxed grain structure, while the grains of annealed high-strength Ti + P-IF steel are long and narrow, which means the recrystallization has not started. Therefore, a beneficial texture could not develop.

The size of precipitates is related to the order of their formation and annealing temperature. The precipitates in the steel dissolve in order, depending upon individual solubility products. Standard Gibbs free energy determines the stability of a compound. The greater the standard Gibbs free energy, the stabler the precipitate. According to thermodynamic data [16], the order of stability of precipitates in Ti-IF steels is TiN > TiS > $Ti_4C_2S_2$; hence, TiN precipitates before TiS, which precipitates before $Ti_4C_2S_2$. Ti and N atoms form a strong bond; the TiN compound forms

Fig. 1 Mechanical properties of experimental steels

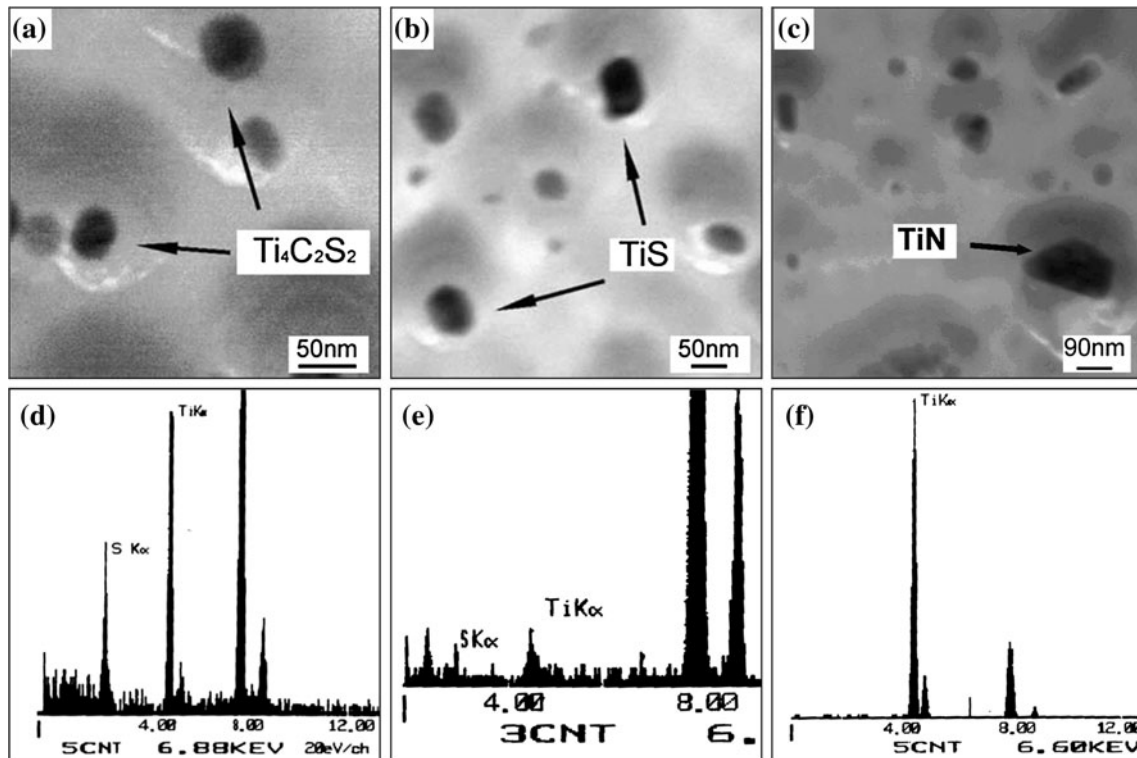Fig. 2 Annealed microstructures of experimental steels

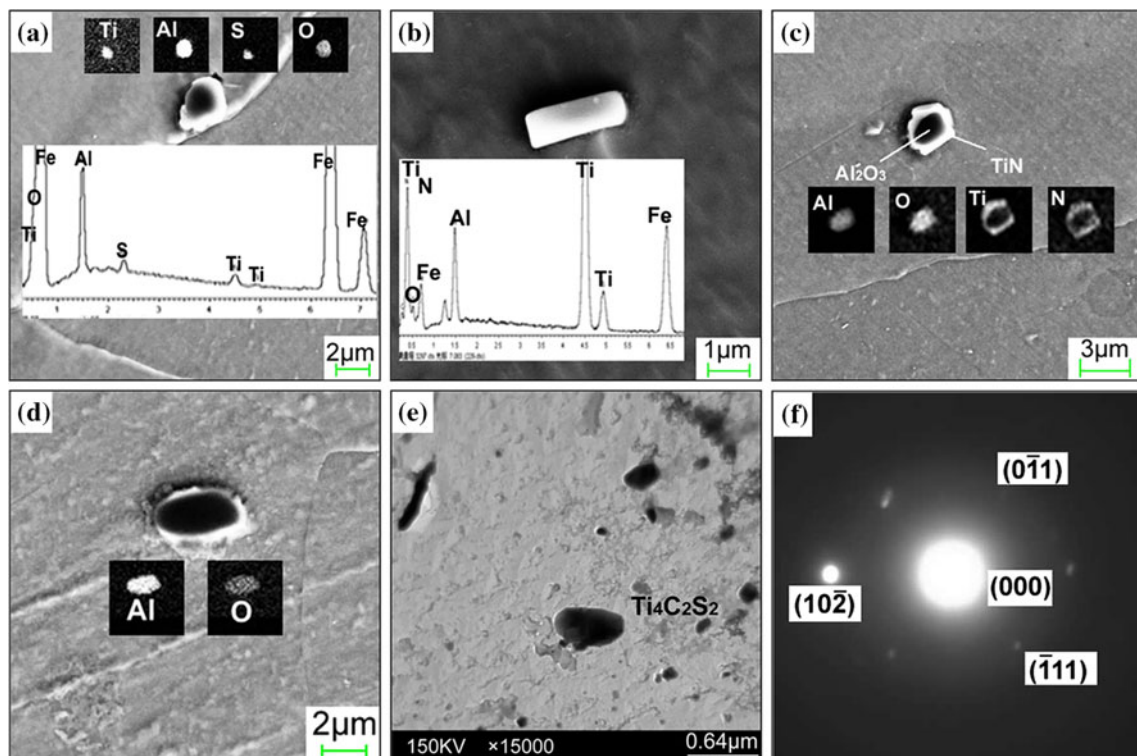Fig. 3 Precipitates in IF steels by TEM analysis

Fig. 4 SEM and TEM analyses of ferritic-rolled, P-added high-strength Ti + P-IF steels sheets: (a) morphology, elements' distribution, and EDS of Al_2O_3 and TiS; (b, c) morphology, elements' distribution, and EDS of Al_2O_3 and TiN; (d) Elements' distribution in Al_2O_3; (e, f) morphology and electron diffraction pattern of $Ti_4C_2S_2$ particle by TEM
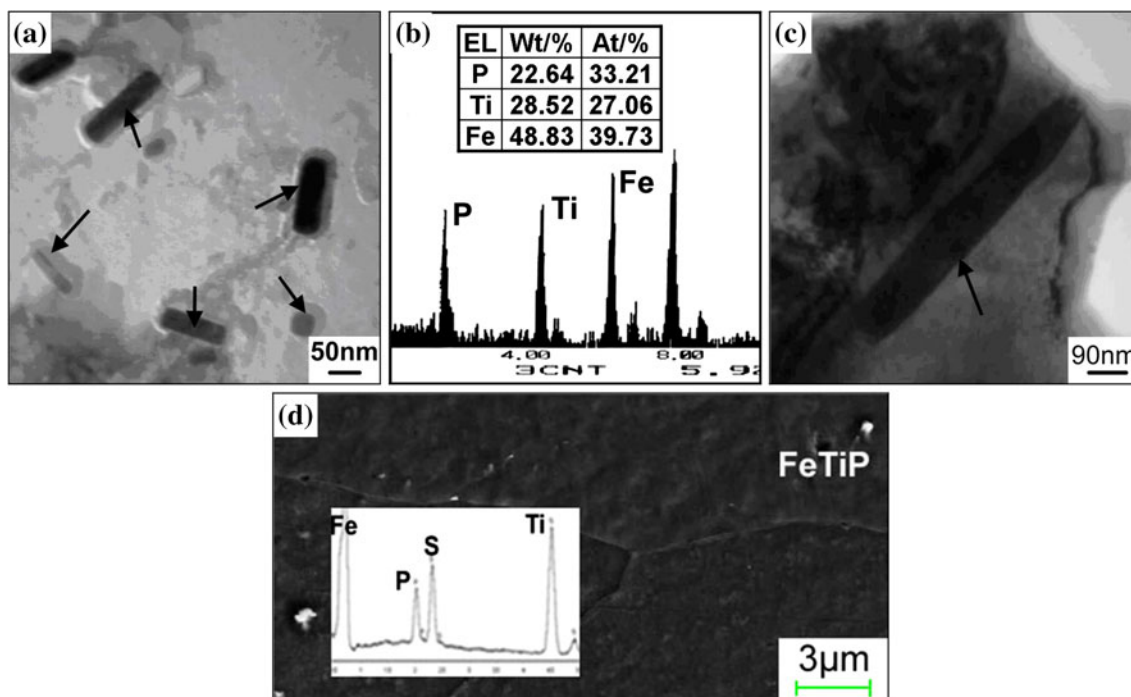
Fig. 5 FeTiP phase in high-strength Ti + P-IF steel by TEM (**a**, **b**, **c**) and SEM (**d**)
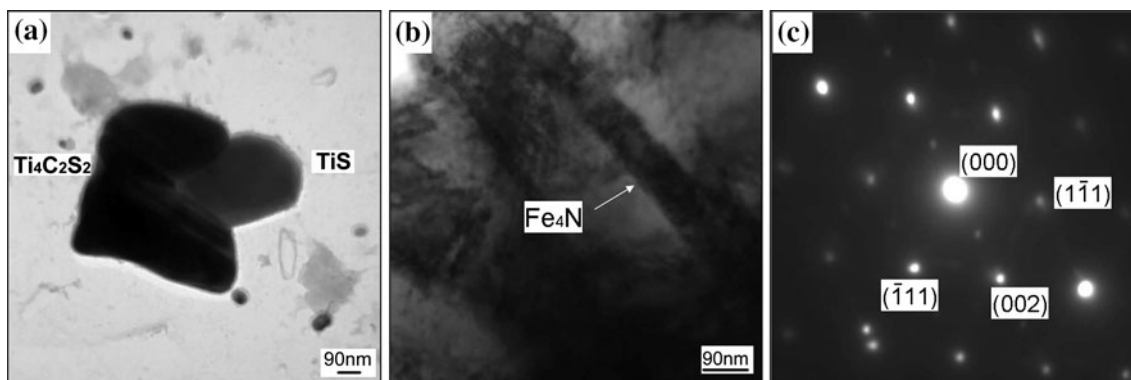

Fig. 6 Other precipitates in high-strength Ti + P-IF steel by TEM

Fig. 7 $\varphi_2 = 45°$ section ODF maps of Ti-IF steels and high-strength Ti + P-IF steel sheets before annealing. (**a**) Ti-IF steel and (**b**) high-strength Ti + P-IF steel
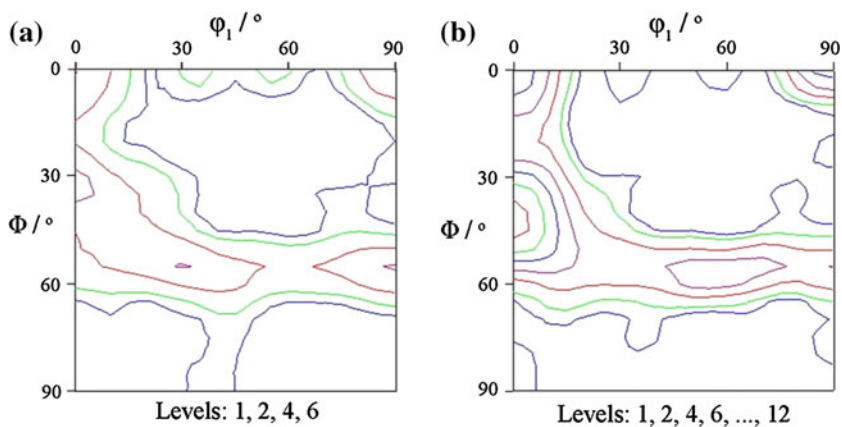
Fig. 8 $\varphi_2 = 45°$ section ODF maps of annealed Ti-IF steels and high-strength Ti + P-IF steel sheets. (**a**) Ti-IF steel, and (**b**) high-strength Ti + P-IF steel
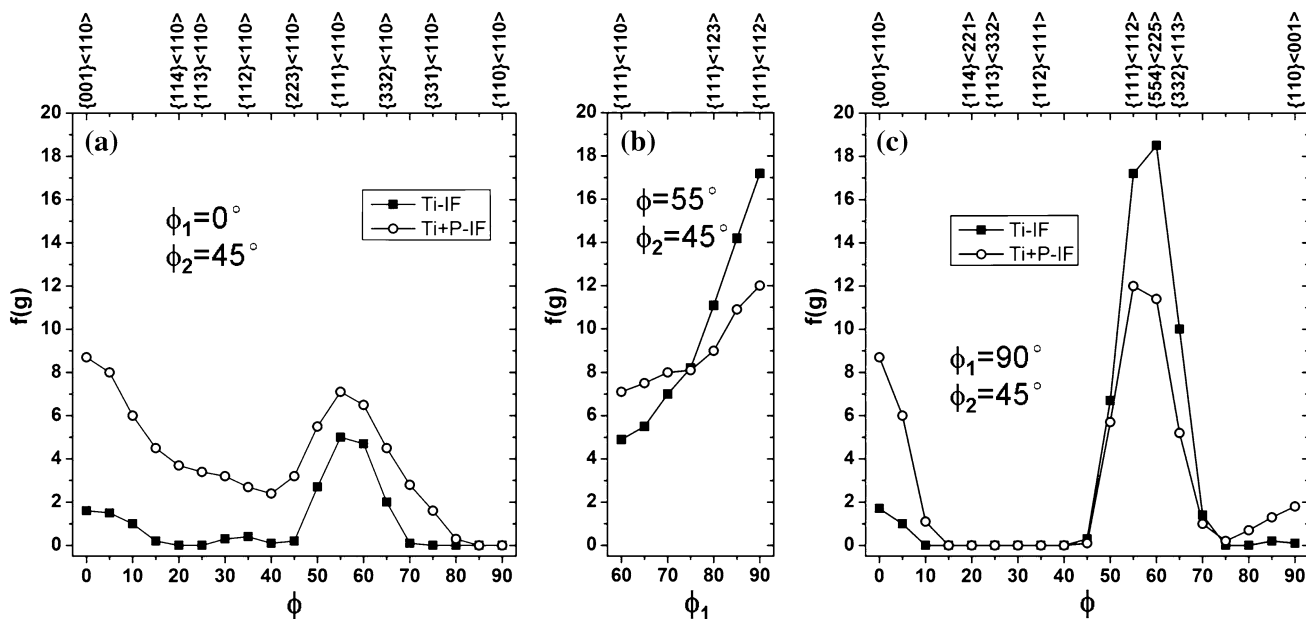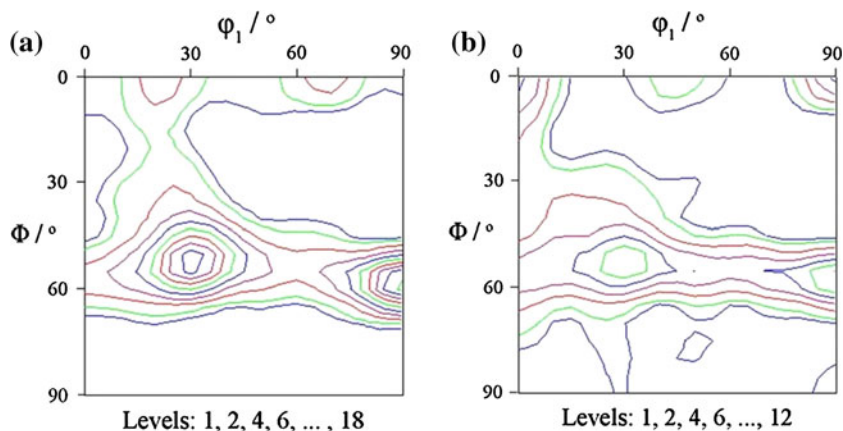

Fig. 9 Orientation density change along (**a**) α, (**b**) γ, and (**c**) ε fibers for ferritic-rolled and annealed IF steel and high-strength Ti + P-IF steel sheets

at high temperature and grows during cooling. Therefore, TiN precipitates first at the highest temperature and keeps growing in the following rolling and annealing process. This is why TiN is larger than other particles, approximately 200 nm, as shown in Fig. 3.

TiS is the main sulfide at high temperature, while $Ti_4C_2S_2$ predominates at low temperature, as it is stabler than TiS [21]. The precipitates are rectangular, square, round, or curved. According to energy dispersive spectroscopy (EDS) analysis, rectangular and square particles are mainly TiN, whereas round and curved particles are mainly TiS and $Ti_4C_2S_2$. Carbon was not detected in the EDS data, and so TiS and $Ti_4C_2S_2$ are distinguished by the Ti and S signals. When the atom ratio Ti:S = 1, the particle is TiS, as shown in Fig. 3(b) and (e); when the atom ratio Ti:S = 2, the particle is $Ti_4C_2S_2$, as shown in Fig. 3(a) and (d).

Figure 4 shows SEM and TEM micrographs of warm-rolled high-strength Ti + P-IF steels sheets. Al and Si are combined with O atoms as an oxide to preclude O atoms from entering solid solution. $Ti_4C_2S_2$ particles play an important role in eliminating C and N atoms from solid solution [1]. The existence of Al_2O_3 is attributed to the stage of melting, during which Al was added to combine with O. Al_2O_3 became the nucleation core of other particles such as TiN, as illustrated in Fig. 4(c).

Figure 5 shows the FeTiP precipitate in high-strength Ti + P-IF steel. The particles are rectangle, square and rod shaped, and their sizes are from 20 to 200 nm. Researchers [22] have shown that FeTiP phase precipitates when the Ti + P-IF steel is held at 700–800 °C for a long time. This has a deleterious effect on formability. Yoshinaga et al. [23]. concluded that when the solid-solution hardening element P precipitates as a compound, FeTiP blocks

recrystallization and thus decreases the yield strength and tensile strength of the steel, which lowers the r value. Other researchers [2] have shown that FeTiP harms strength and the r value and FeTiP precipitation at 600–800 °C should be avoided.

Formation of FeTiP reduces Ti atoms in solid solution. Research has shown that with 0.02 wt% C, $Ti_4C_2S_2$ increases as S content decreases, and TiS increases as S content increases [23]. With 0.008 wt% S, $Ti_4C_2S_2$ increases with an increase in Ti content; TiS increases with the decrease of Ti. Under these conditions, $Ti_4C_2S_2$ transforms to TiS to provide Ti atom for FeTiP. Figure 6(a) shows the compound precipitates of $Ti_4C_2S_2$ and TiS; TiS nucleates and grows on one side of $Ti_4C_2S_2$. Hua et al. and Carabajar et al. [24, 25] refer to the $Ti_4C_2S_2$–TiS–$Ti_4C_2S_2$ type as a "sandwich-like" composite structure. The formation of FeTiP leaves less Ti available for combination with N; additionally, N atoms leave interstitial solid solution in Fe matrix by forming Fe_4N, as shown in Fig. 6(b).

It can be seen from Figs. 7–9 that, after annealing, a strong γ texture and its $\{554\}\langle225\rangle$ component replace most of the α texture in Ti-IF steel. In Ti + P-IF steel, there is residual α texture, and its γ texture is weaker than that in Ti-IF steel. This reflects the fact that the r value of Ti-IF steel is 1.75, and the r value of high-strength Ti + P-IF steel is 1.38. In addition, in high-strength Ti + P-IF steel, recrystallization is not complete, because of the existence of P. FeTiP particles block the formation of {111} orientation grains. This is why the {111} texture is weaker in high-strength Ti + P-IF steel than that in ordinary Ti-IF steel. As a consequence, the r value is smaller.

Conclusions

The effect of P addition to IF steel has been studied with mechanical testing, SEM, TEM, and EBSD. Both the tensile strength and yield strength of high-strength Ti + P-IF steel are much higher than that of ordinary Ti-IF steel because of the strengthening effect of P. Tensile strength rises from 245 to 325 MPa, and yield strength rises from 105 to 165 MPa. However, deep drawability is impaired. Elongation declines from 50 to 40%. The n value and r value drop from 0.31 and 1.75 to 0.25 and 1.38, respectively.

Recrystallization is not complete in high-strength Ti + P-IF steel. A beneficial texture could not nucleate and grow sufficiently to influence formability. This is the main reason for poorer formability of characteristics of high-strength Ti + P-IF steel, when compared with ordinary Ti-IF steel.

The solid-solution hardening effect of P raised the strength of steel, but the FeTiP phase causes a decrease of

r value. FeTiP particles block the formation of {111} orientation grains during annealing, which leads to weaker {111} texture and a lower r value after annealing. Another reason for the damage of formability by P is that FeTiP precipitation leaves less Ti in solid solution to tie-up interstitial atoms, such as N.

References

1. P. Ghosh, B. Bhattacharya, R.K. Ray, Comparative study of precipitation behavior and texture formation in cold rolled-batch annealed and cold rolled-continuous annealed interstitial free high strength steels. Scr. Mater. **56**(8), 657–660 (2007)
2. S.S. Zhao, W.M. Mao, Y.N. Yu, Precipitation behavior of FeTiP phase in high strength IF steel. J. Univ. Sci. Technol. Beijing **7**(3), 197–203 (2000)
3. X.M. Chen, S.H. Song, L.Q. Weng et al., Relation of ductile-to-brittle transition temperature to phosphorus grain boundary segregation for a Ti-stabilized interstitial free steel. Mater. Sci. Eng. A **528**(28), 8299–8304 (2011)
4. X.L. Song, Z.X. Yuan, J. Jia et al., Phosphorus segregation behavior at the grain boundary in a Ti-IF steel after annealing. Scr. Mater. **63**(4), 446–448 (2010)
5. P. Ghosh, C. Ghosh, R.K. Ray et al., Precipitation behavior and texture formation at different stages of processing in an interstial free high strength steel. Scr. Mater. **59**(3), 276–278 (2008)
6. M.R. Barnett, J.J. Jonas, P.D. Hodgson, A comparison between the recrystallization behaviors of warm and cold rolled ferrite. Iron Steelmak. **23**(9), 39–45 (1996)
7. J.J. Jonas, Effects of shear band formation on texture development in warm-rolled IF steels. J. Mater. Process. Technol. **117**, 293–299 (2001)
8. X.J. Guan, Y. Li, Z.C. Wang, Research on precipitation of hot rolled Ti-IF steels in the ferrite region. Iron Steel **39**(9), 58 (2004). (in Chinese)
9. Y.H. Guo, Z.D. Wang, J.S. Xu, G.D. Wang, X.H. Liu, Texture evolution in a warm-rolled Ti-IF steel during cold rolling and annealing. J. Mater. Eng. Perform. **18**(4), 378–384 (2009)
10. Z.D. Wang, Y.H. Guo, G.D. Wang et al., Recrystallization texture characteristic and drawability of a warm rolled and cold rolled interstitial-free steel. J. Mater. Eng. Perform. **15**(6), 646–650 (2006)
11. Y.H. Guo, Z.D. Wang, G.D. Wang, Texture evolution during annealing in warm-rolled and cold-rolled Ti-IF steel. J. Mater. Eng. Perform. **20**(3), 417–421 (2011)
12. A. Oudin, P.D. Hodgson, M.R. Barnett, EBSD analysis of a Ti-IF steel subjected to hot torsion in the ferritic region. Mater. Sci. Eng. A **486**(1–2), 72–79 (2008)
13. A.O. Humphreys, D. Liu, M.R. Toroghinejad, E. Essadiqi, J.J. Jonas, Warm rolling behaviour of low carbon steels. Mater. Sci. Technol. **19**, 709–714 (2003)
14. G.H. Akbari, C.M. Sellars, J.A. Whiteman, Microstructural development during warm rolling of and IF steel. Acta Mater. **45**(12), 5047–5058 (1997)
15. G.H. Akbari, C.M. Sellars, J.A. Whiteman, Quantitative characterization of substructural development during warm working of an interstitial free steel. Mater. Sci. Technol. **16**(1), 47–54 (2000)

16. X.H. Yang, D. Vanderschuseren, J. Dilewijns et al., Solubility products of titanium sulphide and carbosulphide in ultra-low carbon steels. ISIJ Int. **36**(10), 1286–1294 (1996)

17. W.M. Guo, Z.C. Wang, S. Liu et al., Effects of lubricate condition on microstructure and mechanical properties of ferritic rolled high strength IF steel. Mater. Sci. Technol. **19**(4), 59–63 (2011). (in Chinese)

18. ISO 6892-1: 2009; Metallic materials—tensile testing at ambient temperature

19. ISO 10113: 2006; Metallic materials—sheet and strip—determination of plastic strain ratio

20. ISO 10275: 2007; Metallic materials—sheet and strip—determination of tensile strain hardening exponent

21. S.V. Subramanian, M. Prikryl, B.D. Gaulin, Effect of precipitate size and dispersion on Lankford values of titanium stabilized interstitial-free steels. ISIJ Int. **34**(1), 61–69 (1994)

22. D.L. Xiong, W.M. Mao, Precipitation hardening of FeTiP phase in P-added high strength IF steel. J. Univ. Sci. Technol. Beijing **22**(4), 350–353 (2000). (in Chinese)

23. N. Yoshinaga, K. Ushioda, S. Akamatsu et al., Precipitation behavior of sulfides in Ti-added ultra low-carbon steels in austenite. ISIJ Int. **34**(1), 24–32 (1994)

24. M. Hua, C. Garcia, A.J. Deardo, Precipitation behavior in ultra-low-carbon steels containing titanium and niobium. Metall. Mater. Trans. A **28**(9), 1769–1780 (1997)

25. S. Carabajar, J. Merlin, V. Massardier et al., Precipitation evolution during the annealing of an interstitial-free steel. Mater. Sci. Eng. A **281**(122), 132–142 (2000)